Sequestration of Landfill Gas Emissions using Basic Oxygen Furnace Slag: Effects of Moisture Content and Humid Gas Flow Conditions

Krishna R. Reddy, F.ASCE
Professor, University of Illinois at Chicago, Department of Civil & Materials Engineering, 842 West Taylor Street, Chicago, IL 60607, USA; e-mail: kreddy@uic.edu (Corresponding author)

Archana Gopakumar, S.M. ASCE
Graduate Research Assistant, University of Illinois at Chicago, Department of Civil & Materials Engineering, 842 West Taylor Street, Chicago, IL 60607, USA; e-mail: agopak2@uic.edu

Jyoti K. Chetri, S.M.ASCE
Graduate Research Assistant, University of Illinois at Chicago, Department of Civil & Materials Engineering, 842 West Taylor Street, Chicago, IL 60607, USA, e-mail: jkc4@uic.edu

Girish Kumar, S.M.ASCE
Graduate Research Assistant, University of Illinois at Chicago, Department of Civil & Materials Engineering, 842 West Taylor Street, Chicago, IL 60607, USA; e-mail: gkumar6@uic.edu

Dennis G. Grubb, M.ASCE
President, Fugacity LLC, 126 Veronica Lane, Lansdale, PA 19446, USA;
e-mail: dggrubbphdpe@gmail.com

Manuscript Submitted to:
Journal of Environmental Engineering, ASCE

July 15, 2019

ABSTRACT: Fugitive methane (CH_4) and carbon dioxide (CO_2) emissions from municipal solid waste (MSW) landfills constitute one of the major anthropogenic sources of greenhouse gas (GHG) emissions. In this regard, several researchers have focused on developing biocovers which are primarily aimed at reducing CH_4 emissions from MSW landfills. Although these studies have been successful in reducing the CH_4 emissions, the continuous CO_2 emissions due to microbial CH_4 oxidation and MSW decomposition remain a major concern. In this study, the CO_2 sequestration potential of basic oxygen furnace (BOF) steel slag subjected to simulated landfill gas (LFG) conditions was examined to alleviate CO_2 emissions from landfills while also promoting beneficial use of BOF slag. Several series of batch experiments were performed at typical ambient conditions with varying moisture contents to evaluate the CO_2 removal capacity of BOF slag. Small-scale column experiments were also performed simulating various LFG flow conditions such as dry and humid LFG, and continuous and intermittent LFG flow into the column. The results from the batch experiments showed that moisture is requisite for initiation of carbonation reactions in BOF slag; however, there was no definitive trend or an optimum moisture content that could be defined for the range of moisture contents tested. The CO_2 removal rate appeared to have a two-step mechanism: initial rapid CO_2 removal followed by gradual removal of CO_2. The CO_2 removal capacity of BOF slag was found to be 350 mg/g and 155 mg/g of CO_2 under humid and dry LFG conditions, respectively. The total residual lime/portlandite, which is readily available at slag surface, appears to be responsible for the instantaneous carbonation of CO_2. In the long term, the CO_2 removal exceeded the theoretical capacity of total residual lime/portlandite content, which was likely associated with the leaching of other reactive minerals such as larnite (Ca_2SiO_4). An appreciable CH_4 removal by BOF slag (120 mg/g and 40 mg/g under humid and dry conditions, respectively) was observed.

55

56 **Keywords:** MSW landfill, biocover, LFG emissions, BOF slag, CO_2 sequestration.

57

INTRODUCTION

Biodegradation of the waste in landfills results in LFG emissions which comprise of approximately 50% CH_4, 50% CO_2, trace amounts of hydrogen sulfide (H_2S) and other non-methanogenic organic compounds. In the U.S., LFG emissions are one of the major anthropogenic sources of GHG emissions (US EPA, 2018). LFG emissions are addressed by active gas extraction systems installed at landfills; however, these systems are not 100% efficient due to the limited radius of influence of each gas extraction well (Spokas et al. 2006). In 2016, fugitive emissions of LFG into the atmosphere were estimated at ~86.6 million metric tons of CO_2 equivalents per year (US EPA, 2017). Fugitive CH_4 emissions from landfills pose a major problem due to high global warming potential (GWP) of CH_4 of 28- 36 over 100 years (US EPA 2015), with emission rates as high as 10,000 mg CH_4 m^{-2} d^{-1}, of which only 4-50% undergoes oxidation while passing through landfill covers (Spokas et al. 2006).

Several studies address alternate cover systems, known as biocovers, that leverage the microbial CH_4 oxidation that occurs in the landfill cover soils due to the presence of methanotrophs. Biocovers that incorporate biologically-amended soils can enhance methanotrophic activity leading to higher CH_4 oxidation rates (Sadasivam and Reddy 2014). However, the organic materials commonly used as biocover amendments such as dewatered sewage sludge, compost, and biosolids consist of unstable/degradable organic carbon that eventually add to LFG emissions, thus exacerbating the situation. Alternatively, recent studies investigating the use of biochar as an organic amendment in the biocovers showed enhanced methanotrophic activity and CH_4 oxidation (Yargicoglu and Reddy 2015, 2017). Biochar is a solid product derived from pyrolysis or gasification of organic matter under low oxygen

conditions. It contains more stable forms of organic carbon (compared to compost and biosolids), high internal porosity, high water-holding capacity and high specific surface area making it a good host media for bacteria to thrive and proliferate (Yargicoglu and Reddy 2015, 2017).

Although CH_4 emissions can be mitigated/controlled through the use of biochar-amended soils, there are still uncontrolled emissions of CO_2 due to CH_4 oxidation and prevailing waste decomposition. Complementing the CH_4 oxidation with CO_2 sequestration in biocovers has the ability to result in "zero-emissions" from landfills. Accordingly, carbon capture and storage (CCS) techniques using alkaline industrial by-products such as basic oxygen furnace (BOF) slag adds an important dimension to potentially sustainable solutions to this global challenge. The free-lime (CaO), portlandite [$Ca(OH)_2$] and oxides/silicate minerals containing divalent cations (Ca, Mg, Fe) in BOF slag can promote conversion of CO_2 to stable carbonates.

Historically, studies have been conducted to analyze the CO_2 removal potential of BOF slag for on-site carbon capture at industries such as steel production facilities, to optimize reaction parameters (Huijgen et al. 2005; Su et al. 2016), and to purify raw biogas to natural gas levels (Sarperi et al. 2014). Huijgen et al (2005) reported a maximum carbonation degree of 74% of the Ca content for powder slag (< 38μm) and highlighted particle size and reaction temperature as the factors affecting reaction rate. However, the conditions under which BOF slag carbonation was evaluated in these studies do not relate to its potential use under landfill cover conditions. For example, Huijgen et al. (2005) and Su et al. (2016) conducted experiments on BOF slag under stirred powdered and slurry conditions which are considered most conducive for accelerated carbonation, whereas the landfill cover soils mostly exist under unsaturated and static conditions with larger diameter particle sizes. According to a Midwest US landfill temperature study completed by Yesiller and Hanson (2003), temperatures only reach 23°C in the landfill

104 cover soil during summer, whereas industrial carbon capture studies are on the order of 100°C
105 (Huijgen et al. 2005, Su et al. 2016) with elevated pressures (20 bar and 250 kg/cm^2). Sarperi et
106 al. (2014) conducted carbonation experiments at conditions that were closest to landfill
107 conditions with unsaturated slag samples at 20°C. Sarperi et al (2014) showed a CO_2 removal
108 capacity of 72 g CO_2/kg BOF slag corresponding to a 9% conversion of CaO in a column
109 experiment under ambient conditions using fine BOF slag (0-1 mm).
110 Researchers so far have focused on the mineral carbon sequestration using steel slags
111 under optimized conditions to accelerate the carbonation process. Limited studies have focused
112 on CO_2 sequestration by BOF slag under ambient conditions and none of the previous studies
113 have explored the CO_2 sequestration potential of the BOF slag under landfill conditions. This
114 paper presents a first study on the use of BOF slag as an amendment to the landfill cover soil
115 with the specific purpose of CO_2 sequestration under landfill conditions.
116 The objectives of the current study are: (1) to quantify the CO_2 sequestration potential of
117 BOF slag and other cover materials (soil and biochar) exposed to synthetic LFG under ambient
118 conditions; (2) to examine the CO_2 sequestration mechanism of the BOF slag; and, (3) to assess
119 the effect of process variables such as moisture content, gas composition and gas flow conditions
120 on the CO_2 sequestration potential of the slag. Batch experiments were conducted with BOF slag,
121 biochar and a cover soil with synthetic LFG to determine the CO_2 removal mechanisms and the
122 carbonation kinetics at unsaturated moisture conditions and normal atmospheric temperature
123 pertinent in landfill covers. Column experiments were also conducted to determine the
124 breakthrough curve and analyze the CO_2 removal behavior of the BOF slag tested.
125
126 **MATERIALS AND METHODS**

Materials

The materials studied included BOF slag, soil, and biochar. The crushed and screened BOF slag with a top sieve size of 10 mm (3/8 inches) was obtained from Indiana Harbor East Steel Mill (supplied by the Phoenix Services, LLC). The soil was collected from Zion Landfill, IL, from the interim cover placed over MSW. The BOF slag and cover soils were collected manually using shovels and collected in clean 5-gallon buckets. The buckets were immediately sealed with air tight lids to avoid moisture loss. The biochar used in the experiments was acquired from a commercial vendor and it was produced by gasification of waste wood (pinewood) at 570°C as described by Yargicoglu et al. (2015).

The specific gravity of the three materials was determined in accordance to ASTM D854. ASTM D422 was followed to determine the grain size distribution of each media, while Atterberg limits of soil were determined as per ASTM D4318. Hydraulic conductivity and water holding capacity (WHC) were determined according to the ASTM D2434 (for biochar and slag) and ASTM D2980 (for all media), respectively. Hydraulic conductivity of soil was determined according to ASTM 5084 (Method C, Falling head with rising tail water elevation) using a flexible wall triaxial set up. The soil was sieved through No. 4 sieve, which was compacted at 20% target moisture content using a Harvard miniature setup (Humboldt Mfg. Co., Elgin, Illinois) to a density of 2.11 g/cm^3. The hydraulic conductivity of BOF slag was determined on the sample passing through sieve No. 4, whereas the hydraulic conductivity was conducted on biochar sample as is condition.

Oven-dried (100-110°C for 24 hours) samples (~10 g) of BOF slag, soil and biochar were used to determine the loss-on-ignition (LOI) according to ASTM D2974. The pH and oxidation-reduction potential (ORP) were measured using an ORION Model 720A pH meter (ORION Research, Inc., Beverly, Massachusetts) as per ASTM D4972 and the electrical conductivity (EC) was measured using Corning 311 Conductivity meter (Corning Inc., Corning, New York).

The basic physical, chemical and geotechnical properties of BOF slag, soil and biochar used in this study are summarized in **Table 1**. The grain size distribution of each media is shown in **Figure 1**. The representative sample of BOF slag tested consisted of ~91% sand-sized particles and is classified as SP-SM according to Unified Soil Classification System (USCS). The specific gravity of the BOF slag, soil and biochar were determined as 3.04, 2.65 and 0.65, respectively. The hydraulic conductivity of BOF slag and biochar were both on the order of $\sim 10^{-4}$ cm/s, consistent with typical values for fine sands to loose silt (Holtz and Kovacs 1981). The soil had very low hydraulic conductivity in the order of 10^{-8} cm/s. The WHC values of soil (45.9 w/w), BOF slag (40.5 w/w) and biochar (51.55 w/w) were comparable. BOF slag was observed to be highly alkaline with pH ~12.4. The ORP of all three materials were negative, demonstrating high redox conditions.

The minerals present in BOF slag were determined by X-ray powder diffraction (XRD) and Rietveld quantification analysis. The sample preparation for XRD included grinding of a 3 g sample, which was then spiked with corundum (Al_2O_3) on a 90:10 weight basis in a mixer for 10 min. Standard spike intensity reference was used to determine the amorphous content. Step-scanned XRD data were collected by the Siemens D500 computer-automated diffractometer using Bragg-Brentano geometry. The reference databases for powder diffraction and crystal

structure data were the International Center for Diffraction Data database (ICDD, 2001) and the Inorganic Crystal Structure Database (ICSD, 2010, v.2).

The total elemental content was determined as a result of combined XRF/acid digestion tests. Both Toxicity Characteristic Leaching Procedure (TCLP, EPA 1311) and Synthetic Precipitation Leaching Procedure (SPLP, EPA 1312) leaching tests were conducted on the BOF slag.

Scanning Electron Microscopy (SEM) imaging and analysis was conducted on crushed and air-dried samples of BOF slag before and after carbonation experiments. Images were captured using a JEOL JSM-6320F High Resolution Scanning Microscope operated at 2.5 kV. Further, the elemental composition was determined using an Oxford X-Ray Energy Dispersive Spectrometer (XEDS) fitted with a Hitachi S-3000N Variable Pressure Electron Microscope. The specimens were sputter coated with 20 nm Pt/Pd using Cressington HR208 sputter coater to minimize sample charging.

Batch CO_2 Sequestration Experiments

Batch experiments were conducted using BOF slag, soil and biochar to assess their removal potential for CH_4 and CO_2, as shown in **Figure 2a**. The materials were dried in oven at 100-110 °C for 24 hours before they were used in the batch experiments. The batch experiments were conducted by taking 1 g of dry sample in a 125 ml serum vial (Wheaton Glass, Milville, New Jersey) and adding 0%, 10%, 20%, 30% and 40% (w/w) water (or L/S ratio of 0, 0.1, 0.2, 0.3 and 0.4 L/kg, respectively), at ambient temperature. Each vial was then purged completely with a synthetic LFG mix containing 50% CH_4 and 50% CO_2 (v/v), closed with rubber septa, and

secured tightly with a metal crimp cap. Tests were conducted in triplicate for each water content evaluated. The samples were shaken vigorously before sampling the gas from their headspace. Gas samples were taken and analyzed using SRI 9300 GC (SRI Instruments, Torrance, California) equipped with a thermal conductivity detector (TCD) and CTR-1 column capable of simultaneous analysis of CO_2 and CH_4. For each replicate, 1 ml of gas sample was withdrawn from the vial, and reduced to 0.5 ml before injecting into the GC. This ensured the sample volume was within acceptable limits for the GC and in equilibrium with the atmospheric pressure. A 3-point calibration curve was constructed for the SRI 9300 GC using standard CH_4-CO_2 gas mixtures (Praxair Distribution, Inc., Roosevelt Road, Illinois) at 5%, 25%, and 50% (v/v) concentration before testing the samples.

Two sets of batch experiments were conducted. The first set of batch experiments were conducted with each media at five different moisture conditions contacted with synthetic LFG containing 50% CH_4 and 50% CO_2 (v/v) for a total duration of 24 hours. In the second series of batch tests, only BOF slag samples at a single moisture content (of 40%) were exposed to different gas compositions for extended periods up to 1,850 hours: 50% CH_4 and 50% CO_2 mixture, 99% CH_4 and 1% nitrogen mixture, and 50% CO_2 and 50% nitrogen mixture. These gas mixtures were selected to assess if there were any synergistic effects or interference on the removal of CH_4 and CO_2 when both were present. The gas samples were analyzed from these vials until no further CO_2 removal by BOF slag was detected.

Column CO_2 Sequestration Experiments

Column experiments were conducted to determine the CO_2 transport and removal capacity of the BOF slag using the experimental setup shown in **Figure 2b.** An acrylic glass column (Cole-Parmer, Vernon Hills, Illinois) of 30 cm height and 2.5 cm inner diameter was filled with BOF slag with 10% (w/w) moisture content up to its full length in 2 layers of 15 cm each with light tamping. It was secured with bed support mesh screen, end connections, and screw caps at both ends. PTFE tubing was used to connect all components in the setup. Flow meters (Model No.03216-04, Cole-Parmer, Vernon Hills, Illinois) were installed at both ends of the column to control the influent/effluent gas flow rates. Gas samples were collected from each port at different time intervals until CO_2 removal efficiency reduced to nearly 0% ($C_{OUT}/C_{IN} = 1$). 1 ml of gas sample was collected from each sampling port at different time intervals, reduced to 0.5 ml and analyzed using SRI 9300 GC. Three column tests were conducted as follows and summarized in **Table 2**:

- Column DC was tested under the *dry* continuous inflow gas (50% CH_4 and 50% CO_2) conditions at 12 psi inlet pressure and inlet flow rate of 5-9 ml/min at ambient temperature (23°C).
- Column HC was tested for *humid* continuous inflow gas (50% CH_4 and 50% CO_2) conditions at an inlet pressure less than 6 psi and initial inlet flow rate of 10-12 ml/min at atmospheric temperature. The synthetic LFG was passed through a water cylinder to humidify the inlet gas to the column (**Figure 2b**).
- Column DI was conducted with *dry intermittent* gas (50% CH_4 and 50% CO_2) at 12 psi inlet pressure and inlet flow rate 7-11 ml/min at atmospheric temperature.

Humid inflow gas conditions (HC) were tested to simulate the humid LFG conditions and role of moisture on CO_2 removal, if any. The DC and DI tests were included to evaluate the effects of pulsed flow on CO_2 removal.

RESULTS AND DISCUSSION

Slag Characteristics

Table 3 shows the bulk chemistry and mineralogy of the BOF slag. The bulk chemistry (oxides basis) is within the range reported in the published literature (Yildrim and Prezzi 2011; Grubb et al. 2011, 2013; Chiang and Pan 2017). Most reactive minerals in the order of decreasing reactivity commonly present in BOF slag are CaO, $Ca(OH)_2$ and Ca_2SiO_4 (Huijgen et al. 2005; Sarperi et al. 2014; Caicedo-Ramirez et al. 2018). The CaO and $Ca(OH)_2$ constitute the effective "residual lime" immediately available for reaction with CO_2. In the BOF slag used in this study, ~2% CaO and ~9.5% $Ca(OH)_2$ are present, summing to 11.4-11.7 % residual lime content, along with ~11% Ca_2SiO_4. In addition, ~5% $CaCO_3$ in the form of calcite and vaterite was also measured reflecting the influence of air/water cooling during processing at the steel mill.

The total, TCLP, and SPLP heavy metal concentrations of the BOF slag along with the RCRA limits as per 40 CFR 261 are summarized in **Table 4** for comparison purposes. The results show that all TCLP regulated concentrations are within the RCRA limits, thus the BOF slag is classified as non-hazardous. This observation is consistent with Proctor et al. (2000) in which various slags [BOF, blast furnace (BF) and electric arc furnace (EAF)] from 58 active

steel mills across North America (that contribute to more than 47% of the steel production in North America) were characterized to assess their impact on human and environmental health.

The key features of BOF slag compared to other landfill cover materials tested such as soil and biochar are its high material density and high alkalinity. The high density of the BOF slag is attributed to the iron content (**Table 4**). However, the specific gravity of the BOF slag used (3.04) was much less than that reported for typical BOF slag (~3.5) in literature (Chesner et al. 1998). According to Pan et al. (2013) and Morone et al. (2014) steel slags exhibited lower specific gravity and particle density, respectively, upon carbonation (aging). Ko et al. (2015) also mentioned reduction in density from 3.35 g/cm^3 to 2.21 g/cm^3 upon CaO hydration to $Ca(OH)_2$ and its carbonation. The presence of calcium carbonate polymorphs (calcite and vaterite) as shown in **Table 3** confirms the aging of BOF slag leading to the reduction in material density. The alkalinity and elevated pH associated with BOF slag resulting from its residual lime content and basic silicates were viewed as a major challenge with respect to the viability of bacteria (methanotrophs) to convert CH_4 to CO_2.

Batch Experiments

Effect of Moisture Content on Gas Removal

The 24-hour batch experiments were conducted with soil, BOF slag, and biochar at five different moisture contents by weight: 0%, 10%, 20%, 30% and 40% (L/S of 0, 0.1, 0.2, 0.3 and 0.4 L/kg, respectively) such that the values were within their WHC for typical unsaturated conditions in landfill covers. For each moisture content, the samples were tested in triplicate and the statistical

analysis was performed using ANOVA: single factor tool, comparing CO_2 removal in 24 hour for each moisture content. There was significant difference in the total CO_2 removal by the BOF slag from 0% to 40% moisture, with a confidence level greater than 95% ($p=10^{-8}$). The CH_4 and CO_2 removal was calculated based on the differences in their initial concentrations and the quantities of each gas in the microcosm bottles at each testing interval reported by the GC (in triplicate). **Figure 3a** shows the CO_2 removal capacity of BOF slag was in the range of 53-68 mg/g, versus 10 mg/g and 24 mg/g for soil and biochar, respectively. The CO_2 removal by BOF slag was substantially higher than that of soil and biochar, and moreover appeared to be independent of initial moisture content above 0%. The carbonation under dry conditions was only 5 mg/g (negligibly small) indicating that moisture is a pre-requisite for carbonation. The CH_4 removal in all media was insignificant (<6 mg/g), as implied by **Figure 3b**.

Several studies have emphasized the liquid to solid ratios as one of the process variables influencing the carbonation of BOF slag. Some of these studies are summarized in **Table 5**. However, none were able to establish a particular trend with the effect of moisture content on CO_2 sequestration capacity of BOF slag under their respective experimental conditions. Huijgen et al (2005) analyzed the effect of moisture content on degree of carbonation at L/S ratios ranging from 2-20 L/kg under their experimental conditions. They observed slight decrease in the degree of carbonation with the increase in L/S ratio from 2 to 20 L/kg which was attributed to the increase in ionic strength and higher solubility of Ca. On the other hand, in the study by Su et al. (2016), the degree of carbonation remained nearly constant when the L/S ratio increased from 2 to 10 L/kg but it dropped significantly in dry conditions under their experimental conditions, and thus concluded that water is an essential medium for carbonation of BOF slag. Sarperi et al. (2014) used operating conditions closer to the landfill conditions maintained in the present study.

305 BOF slag powder (0-1 mm) was used to sequester CO_2 from raw biogas at regulated temperature
306 (20°C) and exposed to CO_2/CH_4 gas mixture initially supplied to the BOF slag at various
307 moisture contents ranging from 0 to 0.5 L/kg. The CO_2 removal was monitored by GC and
308 optimum L/S ratio was identified as 0.1 L/kg with carbonation decreasing on either side of 0.1
309 L/kg. The reduction in carbonation at higher moisture content (L/S > 0.2 L/kg) was attributed to
310 the decrease in permeability of gas, limiting the interaction of gas with the slag particles and thus
311 decrease in reaction kinetics.

312 **Figure 4a** shows the CO_2 and CH_4 removal trends for the BOF slag during the 24-hour
313 batch experiments. The CH_4 removal was negligible and there was no significant change with
314 time. Likewise, CO_2 removal at 0% moisture (L/S = 0) was insignificant. Batch experiments
315 demonstrated the significance of moisture in BOF slag carbonation by the sudden shift of CO_2
316 removal from 5 mg/g under dry conditions to 61 mg/g (average for all moisture contents tested)
317 under moist conditions. Leaching of Ca^{2+} at the surface of slag particles is facilitated by
318 moisture, which forms the rate determining step of the carbonation reaction (Huijgen et al.
319 2005). The initial hydration of free lime and reaction of CO_2 with portlandite forms the initial
320 carbonates. Further, the Ca^{2+} from the Ca-silicates sequentially leach at the surface of the slag
321 particles to react with CO_2 during which it leaves a shell of unreactive, Ca-exhausted SiO_2 rim.
322 The Ca leaching even in the presence of moisture, could be limited by (1) formation of exhausted
323 SiO_2 particle on the slag particle surface, hindering the Ca^{2+} from reaching surface, (2)
324 precipitation layer of $CaCO_3$ on the surface of slag particles, and (3) stirring rate- a continuous
325 stirring enhances the carbonation as it would make more Ca^{2+} available on the surface to react.
326 Accordingly, as reported by Sarperi et al. (2014), an oven-dried slag (L/S = 0) did not exhibit

CO_2 removal (0 g/kg_{BOF}) whereas the intrinsic water in the as-received slag initiated carbonation (24 g/kg_{BOF}), hence highlighting the role of water in accelerated carbonation.

However, a direct relationship between carbonation capacity and moisture content could not be established from the 24-hour batch experiments in this study. Among the various moisture contents tested, the optimum MC for carbonation was found to be 10% (L/S = 0.1 L/kg), removing a maximum of 68 mg/g CO_2. Thereafter, lower CO_2 removal was observed at both 20% (L/S = 0.2 L/kg) and 40% (L/S = 0.4 L/kg) moisture content, with a slight increased CO_2 removal of 63 mg/g at 30% (L/S = 0.3 L/kg) moisture content. The CO_2 removal trends (**Figure 4a)** affirm that while moisture is a crucial factor for accelerated carbonation of BOF slag, it alone cannot alter the extent of carbonation. Other factors such as BOF slag particle size, ambient temperature, and initial CO_2 pressure usually control carbonation rates (Berryman et al. 2015; Su et al. 2016; Ukwattage et al. 2017) and are viewed as the cause of this varying trend. Since the slag sample was taken as-received for the batch experiments, the particle sizes present in the samples varied which could have led to lesser carbonation in samples having high coarse-to-fine particle ratios.

Further, CO_2 removal shows three distinct slopes in the presence of moisture (**Figure 4a**): first (steepest) slope occurred from 0 to 1 hour, second intermediate slope between 1 to 8 hours, and the flattest slope after 8 hours. Rapid carbonation occurred in the first one hour, followed by more gradual removal thereafter. The difference in slopes is attributed to the dissolution kinetics of various Ca containing minerals present in the BOF slag. The initial steep slope suggests the dissolution of readily available minerals [CaO and $Ca(OH)_2$].

Furthermore, the BOF slag sample (<10 mm) with 61±7 mg/g CO_2 removal capacity over the 10-40% moisture content range was successful under normal landfill conditions. The

optimum moisture content for CH_4 oxidation in landfill covers is on the order of 10-20% (Visvanathan et al. 1999; Huber-Humer et al. 2008), hence the carbonation of BOF slag can be operative while maintaining a nominal moisture content for methanotrophic activity.

Maximum Gas Removal and Synergistic Effects of Gas Composition

Long-term batch experiments with different gas mixtures were conducted on BOF slag following the same procedure as the 24-hour batch experiments, except the initial solid BOF slag at an initial moisture content of 40% (L/S = 0.4 L/kg) was exposed to four synthetic LFG mixtures to analyze the potential synergistic effects of CO_2 and CH_4 removal (**Figure 4b**). **Figure 4b** follows a similar CO_2 removal trend as that observed in the 24-hour batch tests (**Figure 4a**). Carbonation was initially rapid, followed by a continuous lower rate of CO_2 removal. The BOF slag exposed to 50-50 CO_2/CH_4 gas mixture showed greater CO_2 removal (~100 mg/g) than that of 50-50 CO_2/N_2 mixture (~84 mg/g), which could be attributed to the difference in partial pressures of different gas mixtures. Above all, the long-term CO_2 sequestration capacity of the BOF slag exposed to 50-50 CO_2/CH_4 was almost double the rate of 24-hour test. The BOF slag sample showed similar CH_4 removal of about 10-11 mg/g regardless of the gas mixture composition which shows that there was no synergistic effects of gas composition on the CH_4 removal by the BOF slag. In contrast, CO_2 removal showed synergistic effects of gas composition. The CH_4 removal fluctuated between 4-10 mg/g which could be attributed to the changes in adsorption on the slag surfaces.

Column Experiments

373

374 ***Dry Versus Humid Gas Injection***

375

376 The DC column was operated continuously with the inlet and outlet gas monitored regular time
377 intervals for CO_2 and CH_4 concentrations. The CO_2 and CH_4 ratios of outlet concentration to
378 inlet concentration (C_{OUT}/C_{IN}) as a function of pore volume (PV) are shown in **Figures 5(a) and**
379 **5(b)**, respectively. The HC column was conducted in a similar manner and the results are also
380 shown in **Figures 5(a) and 5(b)** for comparison for a total of approximately 1800 PV. The
381 corresponding cumulative CO_2 and CH_4 removals are plotted in **Figures 6(a) and 6(b)**. **Figure**
382 **6(a)** shows the results for a shorter test duration and **Figure 6(b)** shows the results for longer test
383 duration.

384 **Figure 5(a)** shows that under DC conditions, the C_{OUT}/C_{IN} for CO_2 is ~ 0 implying 100%
385 removal of CO_2 until 100 PV (with cumulative removal of 42 mg/g CO_2 as shown in **Figure**
386 **6(a)**). After 100 PV, C_{OUT}/C_{IN} increased rapidly to 0.7 at 150 PV. The ratio then gradually
387 increased to ~1 at around 1,553 PV (**Figure 5a**), for a total of ~155 mg/g of CO_2 removed at test
388 termination (**Figure 6b**). For DC conditions, CH_4 was almost always present in the effluent
389 (**Figure 5b**). Up to 100 PV, the C_{OUT}/C_{IN} ratio of CH_4 fluctuated around 0.4, then rapidly
390 increased to ~ 1 after the CO_2 breakthrough (**Figure 5b**), resulting in a cumulative 40 mg/g of
391 CH_4 removal (**Figure 6b**).

392 The CO_2 removal under HC condition followed similar pattern as DC condition until
393 breakthrough for a removal of ~ 42 mg/g of CO_2 at 100 PV (**Figures 5a and 6a**). After 100 PV,
394 the CO_2 C_{OUT}/C_{IN} increased rapidly to 0.6 at 200 PV (~ cumulative 58 mg/g) showing a removal
395 efficiency of 40%. The CO_2 C_{OUT}/C_{IN} continued as 0.6 until termination of the HC column test

(Figure 5). The corresponding inflow PV was 1,800 (213 hours) and the CO_2 removal was ~350 mg/g **(Figure 6b)**. The HC column did not reach $C_{OUT}/C_{IN} = 1$ until termination, illustrating more potential to remove CO_2. Surprisingly, HC column also showed considerable amount of CH_4 removal (~118 mg/g) (**Figure 6b**) which could be due to adsorption or some reaction mechanism involved which needs further investigation.

As shown in **Figures 6(a) and 6(b)**, the slope of cumulative CO_2 removal curve under DC column conditions reduces from 0.4 to 0.07 at 100 PV (breakthrough). Cumulative CH_4 removal also followed a similar trend changing from 0.11 to 0.02 after the breakthrough. The cumulative CO_2 removal slope by BOF slag under HC conditions reduces from 0.4 to 0.2 before and after the breakthrough, respectively. A similar slope change in the cumulative CH_4 removal curve was observed from 0.13 to 0.06 before and after breakthrough, respectively.

Intermittent versus Continuous Gas Injection

Column DI was cycled with dry inlet gas using a 9-10 hours ON/14-15 hours OFF schedule. Each time the gas supply was reinstated, a C_{OUT}/C_{IN} similar to the previous cycle was re-established in approximately 45 minutes. **Figures 7(a) and (b)** compare the results of DI column with DC column. **Figure 7a** shows that the DI column exhibited essentially the same behavior as the DC column through 100 PV. Thereafter, the DI results were clustered slightly lower than the DC column data. **Figure 8** shows the cumulative removal of CO_2 which totalled 185 mg/g. **Figure 7b** shows more overlapping performance of the two columns for CH_4 removal, ultimately the DI column removed 50 mg/g (slightly higher than DC condition) as shown in **Figure 8**. The slope of cumulative CO_2 removal curve by BOF slag changed from 0.4 to 0.11 at 100 PV,

whereas the slope of the cumulative removal curve of CH_4 changed from 0.17 to 0.03 after the breakthrough (**Figure 8**).

Mechanisms of CO_2 Removal

The number of pore volumes until CO_2 breakthrough and the corresponding total CO_2 removals were the same for three column experiments (DC, HC and DI) as shown in **Table 6**. However, the PVs and total CO_2 removal at the termination of the column experiments varied. Breakthrough of CO_2 occurred at 100 PV (8,000-8,260 ml of synthetic LFG) for the BOF slag under all three conditions – DC, HC and DI as shown in **Figure 5a** and **7a**. However, carbonation persisted for longer periods under HC conditions compared to DC/DI conditions. The similarity between the performance of DC and DI columns suggest that moist conditions (HC) are critical for sustained CO_2 removal. However, initial breakthrough appears independent of gas conditions (humidity) suggesting the availability of "residual lime" on slag surface is decisive. Also, it can be inferred that the initial moisture content (10%) was sufficient to initiate the carbonation process until breakthrough.

Huijgen et al. (2005) observed $Ca(OH)_2$ was responsible for the instantaneous carbonation of steel making slags, while Sarperi et al. (2014) suggested surface lime (CaO) as equally responsible for instantaneous reactions upon its hydration to form $Ca(OH)_2$. Hence, the instantaneous CO_2 removal of BOF slag until 100 PV is assumed to be the reaction with both CaO and $Ca(OH)_2$ in the as-received BOF slag (11.4 – 11.7 wt%). The leaching of Ca^{2+} ions is thought to be the rate determining reaction step in the surficial carbonation mechanism according

441 to Chiang and Pan (2017) and Huijgen et al. (2005) suggesting moisture accelerates the
442 interstitial Ca availability required for sustained CO_2 sequestration.

443 Stoichiometric CO_2 sequestration of residual lime (11.4-11.7 wt%) amounts to 72 mg/g
444 of CO_2 on a theoretical basis. However, only 42 mg/g of CO_2 (60% of 72 mg/g) was removed at
445 breakthrough, 72 mg/g of CO_2 was removed at around 250-300 PV under HC and 440-450 PV
446 under DC conditions as shown in **Figure 6a**. This suggests that only 60% of the lime was surface
447 or near-surface accessible for instantaneous carbonation until breakthrough. Carbonation of the
448 remaining residual lime was attributed to the leaching of Ca ions from the inner core of the BOF
449 slag particles. The cumulative CO_2 removal persisted beyond the theoretical capacity of residual
450 lime (72 mg/g) as shown in **Figure 6a** which suggests the likelihood of the carbonation of other
451 Ca containing minerals. Other minerals that contain Ca such as Ca-Fe oxides and Ca-Mg-
452 silicates have also been reported to participate in CO_2 removal under variable conditions such as
453 higher moisture availability, finer particle sizes and longer carbonation periods (Huijgen et al.
454 2005; Kasina et al. 2015).

455 CO_2 removal in BOF slag follows two-step reaction mechanism as suggested by the
456 change in slope of cumulative removal curves of HC and DC columns (**Figure 6a**). The initial
457 rapid removal can be attributed to the carbonation of readily available minerals like CaO and
458 $Ca(OH)_2$. The slower CO_2 removal rates may involve leaching of Ca from inner core of slag
459 matrix as well as carbonation of Ca containing minerals with lower solubility rates like Ca
460 silicates (Huijgen et al. 2005). Furthermore, after breakthrough, the slope of HC column is
461 steeper than that of DC (**Figure 6a**) which indicates an increased Ca^{2+} leachability facilitated by
462 the moist conditions in the HC column.

463 Gradual white patchy formation of precipitates was observed in columns during the
464 experiments. Precipitate formation was sporadic until the breakthrough, thereafter progressed
465 uniformly from bottom to top in layers until termination when BOF slag particles were
466 completely covered and cemented together more tightly with white precipitates from
467 carbonation. The initial scattered formation of precipitates throughout the column suggests
468 consumption of surficial residual lime, followed by the progressive carbonation from inlet to
469 outlet.
470
471 ***Mechanisms of CH_4 Removal***
472
473 For all the three conditions tested, removal of CH_4 was low. **Figures 5** to **8** show that the
474 breakthrough and cumulative removal curves of CH_4. The C_{OUT}/C_{IN} ratio of CH_4 remained
475 around 0.4 until 100 PV and then rapidly increased to nearly 0.9 for DC and 0.6 for HC column
476 (**Figure 5a**). The cumulative removal of CH_4 was about one-fourth of CO_2 removal in DC and
477 DI system, while it was one-third of the CO_2 removal in the HC system. Further, the slope of the
478 cumulative CH_4 removal gas followed a similar trend in DC, HC and DI systems, changing from
479 ~0.13 to 0.03 at breakthrough (100 PV).

480 To understand the CH_4 removal, a further in-depth study of chemical reaction
481 mechanisms occurring within the BOF slag matrix is required. It is known from the published
482 literature on steel slag carbonation as well as the XRD results that BOF slag is a complex system
483 that consists of numerous minerals. The basic and amphoteric oxides in the BOF slag form
484 several minerals that have different solubility, reactivity, bonding and other chemical
485 characteristics. It is also a vesicular material with high alkalinity making suitable for metals

immobilization, arsenic removal, and acid mine drainage remediation (Grubb et al. 2011; Grubb and Wazne 2011; Ziemkiewicz and Skousen 1999). Previous studies discussed the influence of oxygen vacancies in iron oxides to adsorb CH_4 and methyl radicals (Cheng et al. 2016) and CH_4 interaction with MgO and alumina (Li et al. 1994a, 1994b), and these metal oxides (FeO, MgO, Al_2O_3) are constituents of BOF slag matrix, suggesting the possibility of CH_4 removal by BOF slag along those routes. Steel slags have been studied by Navarro et al. (2010) to consist of both mesopores and macropores with high specific surface area of 11 m^2g^{-1} providing more adsorptive and reactive area. These properties of steel slag along with slight acidic nature of CH_4 gas may provide a conducive environment for CH_4 adsorption (Chiang et al. 2016).

SEM-EDS Analysis

The SEM images and the SEM-EDS results for as-received and carbonated BOF slag samples are shown in **Figure 9**, whereas the respective quantitative elemental results are summarized in **Table 7**. The EDS result in terms of percentage weight can only be considered as a qualitative method for comparison of steel slag that exhibits surficial and interstitial heterogeneous distribution of elements as it mostly gives the surficial information of very tiny quantity of the crushed sample (<0.5 g) that is considered representative of the larger system.

The image of as-received BOF slag shows the presence of large number of internal pores with a network of needle-like formations observed on the surfaces infringing on the pores as shown in **Figure 9a**. These needle-like formations are suggestive of $CaCO_3$ (Chiang and Pan 2017). In addition, the SEM-EDS spectrum and the quantitative results in **Table 7** confirmed that the original sample tested for the experiments had already started undergoing carbonation during

509 cooling and processing with the presence of carbon (C), oxygen (O) along with calcium (Ca)
510 peaks suggestive of $CaCO_3$.

511 The BOF slag collected from the DC and HC columns at the end of testing were
512 subjected to SEM-EDS analysis to compare the surface and compositional changes due to
513 carbonation. The sample from DI was not analyzed separately due to the similarity in its
514 response to that of DC conditions. Increasing C and O peaks were detected with increasing
515 degrees of carbonation (As-is → DC → HC). The increase in weight percentage of C and O in the
516 carbonated samples are provided in **Table 7**. Both carbonated samples from DC and HC
517 exhibited pore clogging as well as formation of needle-like outgrowths and rhombohedral
518 structures reducing the pore space in the BOF slag matrix as compared to the as-received sample
519 as shown in **Figure 9b** and **9c**. The precipitate formed during the column tests was thus
520 confirmed to be the carbonates with the help of SEM-EDS analysis based on the morphological
521 formations and Ca, C and O peaks.

522

523 **CONCLUSIONS**

524

525 BOF slag was evaluated in this study for its suitability as a material in landfill covers for the
526 mitigation of LFG emissions. Based on the series of batch and column experiments conducted in
527 this study, the following conclusions can be drawn:

528 • BOF slag has a significant capacity to sequester CO_2 under synthetic LFG conditions, and
529 moisture is necessary for the initiation of carbonation reaction. The CO_2 removal process can
530 be divided into (i) instantaneous, and (ii) long-term phases. The instantaneous reaction is
531 attributed to the residual lime content in the BOF slag. The long-term removal is attributed to

the leaching of Ca^{2+} from other reactive silicates which is assisted by the presence of moisture in the system.

- A nominal amount of CH_4 removal by the BOF slag was observed during the batch and column experiments, indicating potential interactions between select oxides and silicates with CH_4.
- The formation of carbonate precipitates in the column experiments did result in hardening of the slag mass within the column, but, there was no significant effect on gas permeability. However, a thorough investigation should be taken to account for potential clogging issues in designing the slag layer thickness, particle size and porosity for the large scale and field scale testing.

ACKNOWLEDGEMENTS

This project is funded by the U.S. National Science Foundation (grant CMMI # 1724773). Phoenix Services, LLC, served as an industrial partner and provided slag samples for this research.

REFERENCES

Berryman, E. J., Williams-Jones, A. E., and Migdisov, A. A. (2015). "Steel slag carbonation in a flow-through reactor system: The role of fluid-flux." *J. Environ. Sci.*, 27(C), 266-275.

A. Caicedo-Ramirez, M.T. Hernandez and D.G. Grubb (2018). "Elution history of basic oxygen furnace slag to produce aklaline water for reagent purposes." Protection and Restoration of the Environment XIV (PREXIV), Greece, July 3-6, 2018.

Cheng, Z., Qin, L., Guo, M., Fan, J. A., Xu, D., and Fan, L. S. (2016). "Methane adsorption and dissociation on iron oxide oxygen carriers: the role of oxygen vacancies." *Phys. Chem. Chem. Phys.*, 18(24), 16423-16435.

Chesner, W. H., Collins, R. J., and MacKay, M. H. (1998). *User guidelines for waste and by-product materials in pavement construction*, Federal Highway Administration (FHWA), FHWA-RD-97-148.

Chiang, W. S., Fratini, E., Baglioni, P., Chen, J. H., and Liu, Y. (2016). "Pore size effect on methane adsorption in mesoporous silica materials studied by small-angle neutron scattering." *Langmuir*, 32(35), 8849-8857.

Chiang, P. C., and Pan, S. Y. (2017). *Carbon dioxide mineralization and utilization*, Springer, Singapore.

Grubb, D. G., Wazne, M., Jagupilla, S. C., and Malasavage, N. E. (2011). "Beneficial use of steel slag fines to immobilize arsenite and arsenate: slag characterization and metal thresholding studies." *J. Hazard. Toxic Radioact. Waste*, 15(3), 130-150.

Grubb, D. G., and Wazne, M. (2011). *Metal immobilization using slag fines*, U.S. Patent Application No. 12/874,079.

Grubb, D. G., Wazne, M., Jagupilla, S., Malasavage, N. E., and Bradfield, W. B. (2013). "Aging effects in field-compacted dredged material: steel slag fines blends." *J. Hazard. Toxic Radioact. Waste*, 17(2), 107-119.

Grubeša, I. N., Barisic, I., Fucic, A., and Bansode, S. S. (2016). *Characteristics and uses of steel slag in building construction*, 1st Ed., Woodhead Publishing.

Gupta, J. D., Kneller, W. A., Tamirisa, R., and Skrzypczak-Jankun, E. (1994). "Characterization of base and subbase iron and steel slag aggregates causing deposition of calcareous tufa in drains". *Transportation Research Record*, (1434).

Holtz, R. D., and Kovacs, W. D. (1981). *An introduction to geotechnical engineering*, 2nd Ed., Prentice-Hall, New Jersey.

Huber-Humer, M., Gebert, J., and Hilger, H. (2008). "Biotic systems to mitigate landfill methane emissions." *Waste Manag. Res.*, 26(1), 33-46.

Huijgen, W. J., Witkamp, G. J., and Comans, R. N. (2005). "Mineral CO_2 sequestration by steel slag carbonation." *Environ. Sci. Technol.*, 39(24), 9676-9682.

Kasina, M., Kowalski, P. R., and Michalik, M. (2015). "Mineral carbonation of metallurgical slags". *Mineralogia*, 45(1-2), 27-45.

Ko, M. S., Chen, Y. L., and Jiang, J. H. (2015). "Accelerated carbonation of basic oxygen furnace slag and the effects on its mechanical properties." *Constr. Build. Mater.*, 98, 286-293.

Li, C., Yan, W., and Xin, Q. (1994a). "Interaction of methane with surface of alumina studied by FT-IR spectroscopy." *Catal. Lett.*, 24(3-4), 249-256.

Li, C., Li, G., and Xin, Q. (1994b). "FT-IR spectroscopic studies of methane adsorption on magnesium oxide." *J. Phys. Chem.*, 98(7), 1933-1938.

Morone, M., Costa, G., Polettini, A., Pomi, R., and Baciocchi, R. (2014). "Valorization of steel slag by a combined carbonation and granulation treatment." *Miner. Eng.*, 59, 82-90.

597 Navarro, C., Díaz, M., andVilla-García, M. A. (2010). "Physico-chemical characterization of
598 steel slag. Study of its behavior under simulated environmental conditions." *Environ. Sci.*
599 *Technol.*, 44(14), 5383-5388.
600 Pan, S. Y., Chiang, P. C., Chen, Y. H., Tan, C. S., and Chang, E. E. (2013). "Ex situ CO_2 capture
601 by carbonation of steelmaking slag coupled with metalworking wastewater in a rotating
602 packed bed." *Environ. Sci. Technol.*, 47(7), 3308-3315.
603 Proctor, D. M., Fehling, K. A., Shay, E. C., Wittenborn, J. L., Green, J. J., Avent, C., Bigham,
604 R.D., Connolly, M., Lee, B., Shepker, T.O., and Zak, M. A. (2000). "Physical and
605 chemical characteristics of blast furnace, basic oxygen furnace, and electric arc furnace
606 steel industry slags." *Environ. Sci. Technol.*, 34(8), 1576-1582.
607 Reddy, K.R., Yargicoglu, E.N., Yue, D., and Yaghoubi, P. (2014). "Enhanced microbial methane
608 oxidation in landfill cover soil amended with biochar." *J. Geotech. Geoenviron. Eng.*,
609 ASCE, 140(9).
610 Sadasivam, B.Y., and Reddy, K.R. (2014). "Landfill methane oxidation in soil and bio-based
611 cover systems." *Reviews in Environ. Sci. Bio/Technol.*, 13(1), 79-107.
612 Sarperi, L., Surbrenat, A., Kerihuel, A., and Chazarenc, F. (2014). "The use of an industrial by-
613 product as a sorbent to remove CO_2 and H_2S from biogas." *J. Environ. Chem. Eng.*, 2(2),
614 1207-1213.
615 Spokas, K., Bogner, J., Chanton, J. P., Morcet, M., Aran, C., Graff, C., Moreau-Le Golvan, L.,
616 and Hebe, I. (2006). "Methane mass balance at three landfill sites: What is the efficiency
617 of capture by gas collection systems?." *Waste Manage.*, 26(5), 516-525.
618 Stolaroff, J. K., Lowry, G. V., and Keith, D. W. (2005). "Using CaO-and MgO-rich industrial
619 waste streams for carbon sequestration." *Energy Convers. Manag.*, 46(5), 687-699.

620 Su, T. H., Yang, H. J., Shau, Y. H., Takazawa, E., and Lee, Y. C. (2016). "CO_2 sequestration
621 utilizing basic-oxygen furnace slag: Controlling factors, reaction mechanisms and V–Cr
622 concerns." *J. Environ. Sci.*, 41, 99-111.
623 Takahashi, T., and Yabuta, K. (2002). *New application of iron and steelmaking slag*, NKK
624 Technical Report-Japanese Edition, 87, 43-48.
625 Ukwattage, N. L., Ranjith, P. G., and Li, X. (2017). "Steel-making slag for mineral sequestration
626 of carbon dioxide by accelerated carbonation." *Measurement*, 97, 15-22.
627 US Environmental Protection Agency (US EPA) (2018). "Landfill methane outreach program
628 (LMOP)." <https://www.epa.gov/lmop/benefits-landfill-gas-energy-projects> (accessed
629 on June 4, 2018).
630 US EPA (2017). "Greenhouse gas reporting program (GHGRP)."
631 <https://www.epa.gov/ghgreporting/ghgrp-waste> (accessed on June 4, 2018).
632 US EPA (2015). "Understanding global warming potentials."
633 <https://www.epa.gov/ghgemissions/understanding-global-warming-potentials>
634 (accessed on June 4, 2018).
635 Visvanathan, C., Pokhrel, D., Cheimchaisri, W., Hettiaratchi, J. P. A., and Wu, J. S. (1999).
636 "Methanotrophic activities in tropical landfill cover soils: effects of temperature,
637 moisture content and methane concentration." *Waste Manag. Res.*, 17(4), 313-323.
638 Yargicoglu, E., Sadasivam, B.Y., Reddy, K.R. and Spokas, K. (2015). "Physical and chemical
639 characterization of waste wood derived biochars." *Waste Manage.*, 36(2), 256-268.
640 Yargicoglu, E. N., and Reddy, K. R. (2015). "Characterization and surface analysis of
641 commercially available biochars for geoenvironmental applications." *IFCEE 2015*, 2637-
642 2646.

643 Yargicoglu, E. N., and Reddy, K. R. (2017). “Effects of biochar and wood pellets amendments
644 added to landfill cover soil on microbial methane oxidation: A laboratory column
645 study.” *J. Environ. Manag.*, 193, 19-31.
646 Yesiller, N., and Hanson, J. L. (2003). “Analysis of temperatures at a municipal solid waste
647 landfill.” Proc., *9th Int. Waste Management and Landfill Symp*., T. H. Christensen et al.,
648 eds., CISA, Italy
649 Yildirim, I. Z., and Prezzi, M. (2011). “Chemical, mineralogical, and morphological properties of
650 steel slag.” *Adv. Civil Eng.,* 2011.
651 Ziemkiewicz, P., and Skousen, J. (1999). “Steel slag in acid mine drainage treatment and
652 control.” *Proc., Annual National Meeting of the Society for Surface Mining and*
653 *Reclamation*, 16, 651-656.

Table 1. Physical, chemical and geotechnical properties of experimentally tested BOF slag, cover soil and biochar

Properties	ASTM Method	BOF Slag	Soil	Biochar
Specific Gravity	D854	3.04	2.65	0.65
Grain Size Distribution:	D422			
Gravel (%)		0	0	45
Sand (%)		90.5	7.2	54
Fines (%)		9.5	92.8	1
D_{50} (mm)		0.47	0.0068	4.3
C_c		0.55	-	0.82
C_u		11.92	-	2.42
Atterberg Limits:	D4318			
Liquid Limit (%)		Non-Plastic	35.0	Non-Plastic
Plastic Limit (%)		-	20.34	-
Plasticity Index (%)		-	14.66	-
USCS Classification	D2487	SP-SM	CL	SP
Water Holding Capacity (w/w)	D2980	40.5	45.9	51.6
Dry Density (g/cm^3)		1.32	2.11	1.15
Hydraulic Conductivity (cm/s)	D2434	4.2×10^{-4}	2.75×10^{-8}	2×10^{-4}
Loss of Ignition (%)	D2974	2.5	4.47	96.71
pH (1:1)	D4972	12.4	7.04	6.5
Electrical Conductivity (mS/cm)	D4972	6.68	0.4	0.8
Redox Potential (mV)	D4972	-317.9	-37.7	-6.3

Table 2. Summary of column experimental conditions

Parameters	**DC**	**HC**	**DI**
Inlet gas:			
Moisture condition	Dry	Humid	Dry
Mode of injection	Continuous	Continuous	Intermittent
Carbon dioxide (%)	50	50	50
Methane (%)	50	50	50
***Column*:**			
Diameter (cm)	2.5	2.5	2.5
Length (cm)	30	30	30
BOF slag mass (g)	189.5	190.8	199.5
BOF slag particle size (mm)	< 4.75	< 4.75	< 4.75
Moisture content (%)	10	10	10
Dry density (g/cm^3)	1.3	1.3	1.38
Porosity (v/v)	0.57	0.57	0.55
Pore volume (ml)	82	82	80
***Flow*:**			
Inlet flow rate (ml/min)	5-9	10-29	7-11
Inlet pressure (psi)	12	< 6	12
Outlet flow rate (ml/min)	1-7	2-21	2-9
Total test duration (min)	17159	103628	17678
Total pore volumes (#)	1553	22357	1882

DC=column with dry gas continuous inflow
HC=column with humid gas continuous inflow
DI= column with dry gas intermittent inflow

Table 3. Mineralogy and bulk chemistry (oxide basis) of BOF slag

Minerals and Oxides	Mineral Formula	Percent Weight
Minerals		
Lime	CaO	2.0-2.2
Portlandite	$Ca(OH)_2$	9.4-9.5
Larnite	Ca_2SiO_4	9.5-11.4
Srebrodolskite	$Ca_2Fe_2O_5$	6.6-7.8
Akermanite	$Ca_2MgSi_2O_7$	0.0-6.4
Magnesioferrite	$MgFe_2O_4$	3.3-3.8
Katoite	$Ca_3Al_2(OH)_{12}$	3.8-4.3
Calcite	$CaCO_3$	2.8-2.9
Vaterite	$CaCO_3$	1.8-2.7
Wuestite	FeO	2.5-2.7
Mayenite	$Ca_{12}Al_{14}O_{33}$	2.7-2.9
Iron magnesium oxide	FeO.76MgO.24O	1.4-1.7
Merwinite	$Ca_3Mg(SiO_4)_2$	0.9-0.9
Periclase	MgO	0.4-0.6
Quartz	SiO_2	0.3-0.4
Brucite	$Mg(OH)_2$	0.3-0.6
Iron	Fe	0.0-0.1
Amorphous material		41.7-50.1
Oxide Basis		
CaO		33.6-33.8
SiO_2		13.3-13.4
Al_2O_3		3.6-3.6
Fe_2O_3		15.4-15.4
MgO		4.6-4.6
SO_3		0.3-0.3
Loss of Ignition (LOI)		8.6-8.6

Table 4. Total, TCLP and SPLP metal concentrations in BOF slag

Constituent	Symbol	Total (mg/kg)	TCLP (mg/L)	SPLP (mg/L)	RCRA Limit (mg/L)
Aluminum	Al	7,600	0.62	0.16	
Antimony	Sb	<0.76	<0.00031	<0.00016	
Arsenic	As	1.3	0.00087	0.00029	5
Barium	Ba	36	0.14	0.12	100
Beryllium	Be	<0.76	<0.00025	<0.00013	
Boron	B	330	0.12	0.027	
Cadmium	Cd	2.5	<0.00028	<0.00015	1
Calcium	Ca	290,000	2,300	800	
Chromium	Cr	1,600	0.011	0.002	5
Cobalt	Co	1.2	0.0034	0.0013	
Copper	Cu	7.4	<0.005	<0.0025	
Iron	Fe	210,000	0.031	0.011	
Lead	Pb	<0.76	<0.00041	<0.00020	5
Magnesium	Mg	65,000	0.077	<0.050	
Manganese	Mn	24,000	0.005	0.00072	
Mercury	Hg	<0.01	<0.00005	<0.00005	0.2
Nickel	Ni	8.2	0.036	0.013	
Potassium	K	<1,500	0.76	0.66	
Selenium	Se	<1.2	0.0047	0.0019	1
Silver	Ag	<0.76	<0.00025	<0.00013	5
Sodium	Na	<1,900	6.4	4.8	
Thallium	Tl	<0.23	<0.00025	<0.00013	
Vanadium	V	1,000	0.0058	0.00078	
Zinc	Zn	59	0.035	0.024	

TCLP = Toxicity Characteristic Leaching Procedure
SPLP = Synthetic Precipitation Leaching Procedure
RCRA = Resource Conservation and Recovery Act

Table 5. Comparison of batch experiments in previous and present study on CO_2 sequestration by steel slag

Reference	Experimental Conditions	Experimental Method	Notes
Huijgen et al. (2005)	**Slag:** Linz Donawitz (LD) steel slag **Moisture:** 2-20 L/kg (L/S ratio) **Reactor:** AISI316 Autoclave Reactor **Stirring rate:** 500 rpm **Grain size:** < 106 µm **Temperature:** 100 °C **Pressure:** 20 bar (continuous CO_2 replenishment) **Reaction time:** 30 min **Analysis method:** Thermogravimetric Analysis (TGA) and acidification	Slag-water mixtures react in a closed reactor at specified conditions. After 30 min, the reactor was cooled, depressurized and opened. The slag-water mixture filtered, slag dried at 50°C in oven overnight and tested.	▪ Optimum L/S: 2 L/kg ▪ Calcium conversion and carbonate content decreased from 60 to 50% and 12.5 to 10.5 (wt%), respectively with increasing L/S from 2 to 20 L/kg, explained by higher ionic strength and higher Ca solubility. Key difference from current study: High temperature, high pressure, finer particle size, higher stirring rate, slurry form, shorter reaction time
Su et al. (2016)	**Slag:** BOF slag **Moisture:** 0 -10 L/kg (L/S) **Reactor:** 20 ml capped (with 7 holes) cell within 500 ml autoclave **Stirring rate:** None **Grain size:** 3.5-2 (mm) **Temperature:** 100 °C **Pressure:** 245 bar **Reaction time:** 24 hours **Analysis method:** TGA	2 g dry slag distributed on cell base, covered with water to reach L/S ratio, positioned in autoclave with dry CO_2 ice, sealed and heated to reaction temperature. Reaction carried until temperature and pressure read 31°C and 75.3 kg/cm^2. The reactor was cooled and depressurized. The slag-water mixture filtered, slag oven dried at 80°C overnight and tested.	▪ Optimum L/S: 2-10 L/kg ▪ Degree of carbonation (wt%) remained nearly constant (16.3%-18.5%) when L/S inreased from 2-10 L/kg Key difference from current study: High temperature, high pressure, slurry form
Sarperi et al. (2014)	**Slag:** BOF slag **Moisture:** 0 - 0.5 L/kg **Reactor:** Atmospheric reactor **Stirring rate:** 300 rpm **Grain size:** 0-1 mm **Temperature:** 20°C(thermo-regulated room) **Pressure:** ND (CH_4/CO_2 gas mixture passed for 5 min at 10 ml/min) **Reaction time:** 6 hours **Analysis method:** Gas chromatography	Slag-water mixture filled into a 100 µm mesh basket (slag basket) and lowered into the reactor, hermetically sealed and gas samples analyzed over time.	▪ Optimum L/S: between 0.05 to 0.2 L/kg (with 65 g/kg$_{BOF}$ CO_2 removal at 0.1 L/kg) ▪ Oven-dried slag (L/S = 0) did not result in any CO_2 removal while the intrinsic water in the as-received slag initiated carbonation, hence highlighting importance of water in accelerated carbonation. Key difference from current study: Finer particle size, shorter reation time, higher stirring rate

Present study	**Slag:** BOF slag **Moisture:** 0 – 0.4 L/kg **Reactor:** 125 ml microcosm bottles **Stirring rate:** Only occassional shaking **Grain size:** <10 mm (3/8") **Temperature:** Room temperature (~23°C, non-regulated) **Pressure:** ND (50% CH_4/50% CO_2 gas mixture purged in vial) **Reaction time:** Test 1: 24 hours; and Test 2: 1850 hours **Analysis method:** Gas Chromatography	1 g dry slag mixed with water to required moisture contents in microcosm bottle, purged to fill with 50% CH_4/50% CO_2 gas mixture and sealed. Gas samples analyzed over time.	▪ Optimum L/S: 0.1 L/kg (with 68 mg CO_2 /g $_{BOF}$ removed at L/S = 0.1 L/kg) ▪ Oven-dried slag (L/S = 0) did not remove any CO_2

Table 6. Cumulative CO_2 removed by BOF slag in column experiments with different flow conditions.

Column	1 PV (ml)	Breakthrough		Termination	
		PV (#)	CO_2 removed (mg/g)	PV (#)	CO_2 removed (mg/g)
DC: Dry & Continuous	82	100	42	1,553	155
HC: Humid & Continuous	82	100	42	1,800	350
DI: Dry & Intermittent	80	100	42	1,882	200

PV= Pore Volume

Table 7. SEM-EDS elemental quantitative results for as-received and carbonated slag from DC and HC column experiments.

Element	Weight (%)		
	As-received	**DC**	**HC**
Ca	55.34	61.57	57.08
Si	9.70	3.92	2.22
Fe	9.69	ND	ND
Mg	2.26	1.87	2.43
Al	1.79	ND	ND
C	5.47	10.73	11.97
O	15.75	21.91	26.29

DC=column with dry gas continuous inflow
HC=column with humid gas continuous inflow
ND=non-detected

Figure Captions

Figure 1. Grain size distribution of BOF slag, soil and biochar

Figure 2. Schematic setup (a) Batch experiment; and (b) Column experiment (humid).

Figure 3. Cumulative (a) CO_2 and (b) CH_4 removal in 24 hours by BOF slag, soil and biochar at different moisture conditions (n = 3).

Figure 4. Cumulative CO_2 and CH_4 removal by BOF slag with time: (a) short-term batch experiments with different initial solid moisture contents; and, (b) long-term batch experiments with different gas mixtures at initial solid moisture content of 40%.

Figure 5. Outlet to inlet concentration ratio of CO_2 (a) and CH_4 (b) under dry (DC) and humid (HC) flow conditions on BOF slag column pore volume basis. Note: MC_i = initial moisture content

Figure 6. Short-term (a) and long-term (b) CO_2 and CH_4 removal under humid (HC) and dry (DC) flow conditions on BOF slag column pore volume basis.

Figure 7. Outlet to inlet concentration ratio of CO_2 (a) and CH_4 (b) under dry continuous (DC) and dry intermittent (DI) flow conditions on BOF slag column pore volume basis.

Figure 8. Comparison of cumulative CO_2 and CH_4 gas removal under dry continuous (DC) and dry intermittent (DI) flow conditions on BOF slag column pore volume basis.

Figure 9. Scanning Electron Microscopy- Energy Dispersive X-Ray Spectroscopy (SEM-EDS) images of BOF slag (a) As-received, (b) DC-Carbonated; and (c) HC-Carbonated (DC-dry gas conditions; HC-Humid gas condition

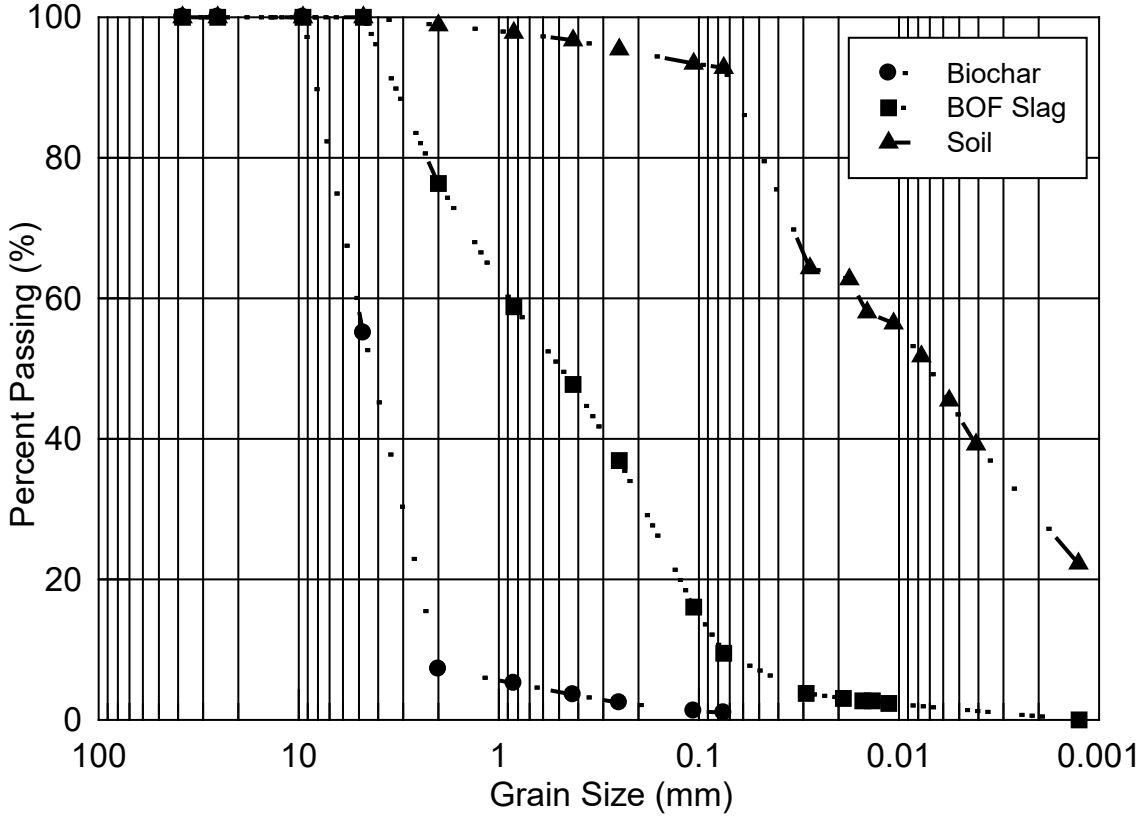
Biochar
BOF Slag
Soil
Percent Passing (%)
Grain Size (mm)
100
80
60
40
20
0
100
10
1
0.1
0.01
0.001

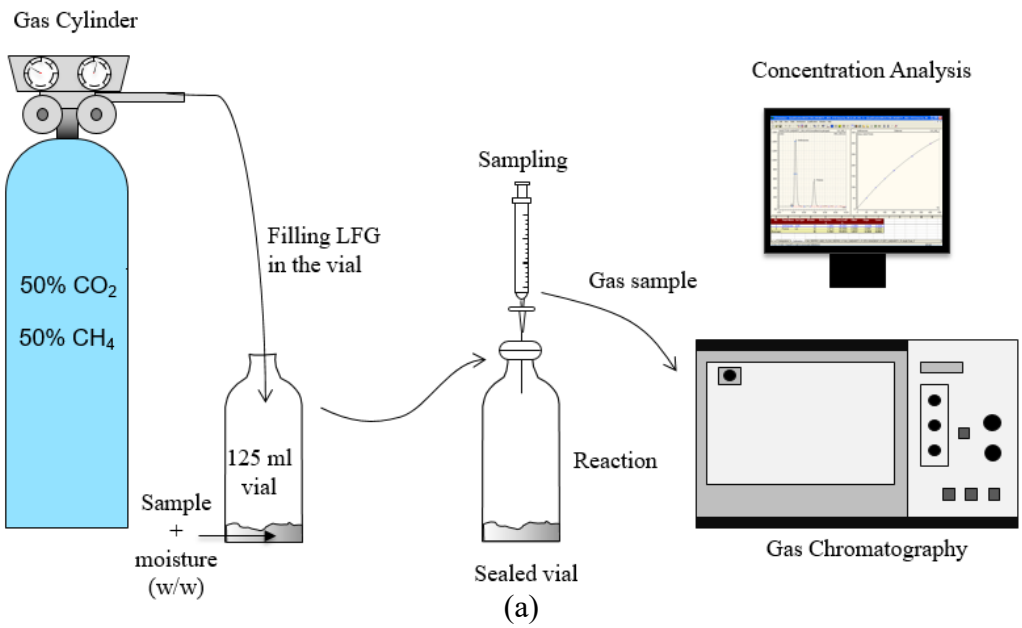
Gas Cylinder
50% CO_2
50% CH_4
Filling LFG in the vial
125 ml vial
Sample + moisture (w/w)
Sampling
Sealed vial
Reaction
Gas sample
Concentration Analysis
Gas Chromatography

(a)

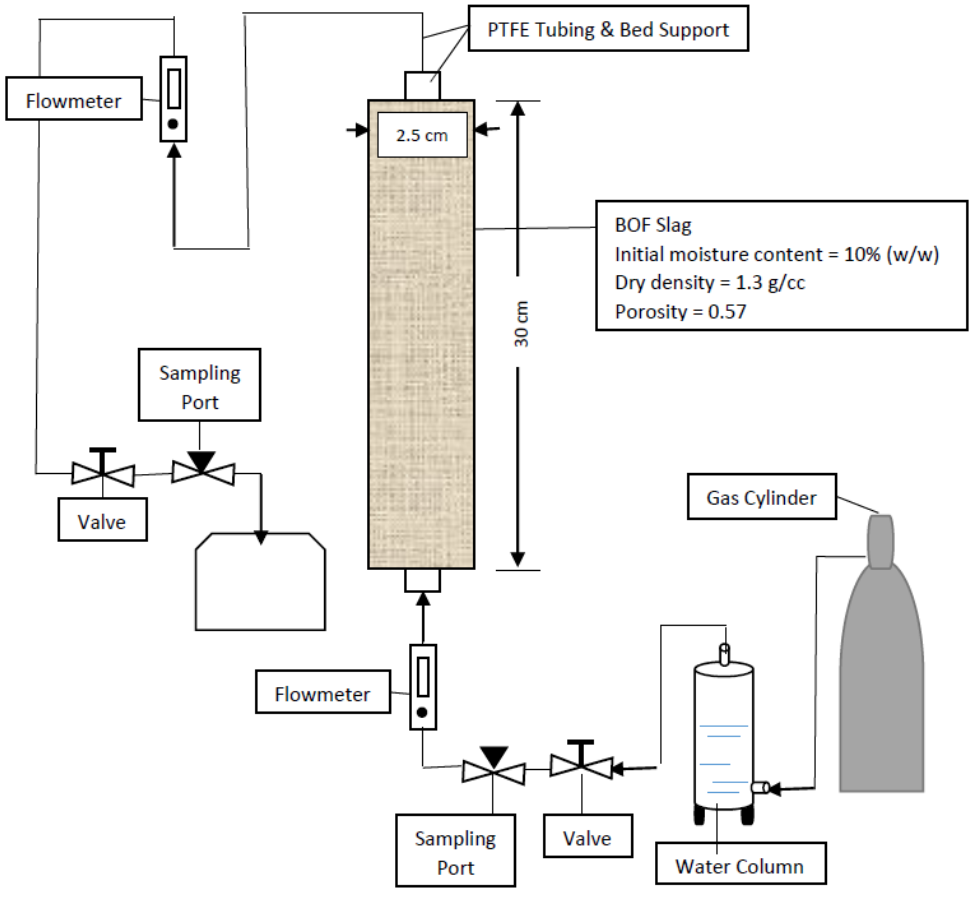
PTFE Tubing & Bed Support
Flowmeter
2.5 cm
BOF Slag
Initial moisture content = 10% (w/w)
Dry density = 1.3 g/cc
Porosity = 0.57
30 cm
Sampling Port
Valve
Gas Cylinder
Flowmeter
Sampling Port
Valve
Water Column

(b)

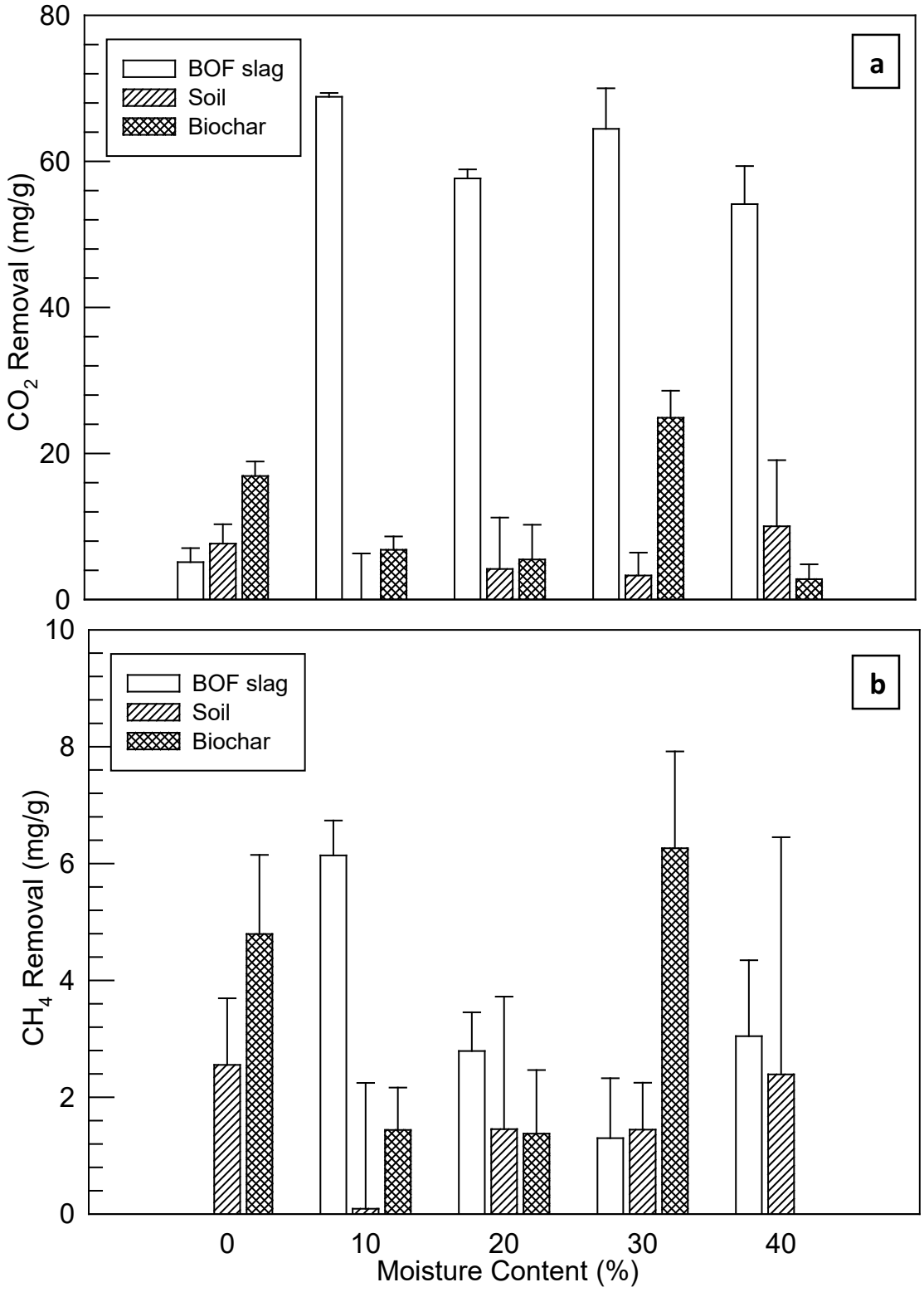
a
BOF slag
Soil
Biochar
CO_2 Removal (mg/g)
0
20
40
60
80
b
BOF slag
Soil
Biochar
CH_4 Removal (mg/g)
0
2
4
6
8
10
0
10
20
30
40
Moisture Content (%)

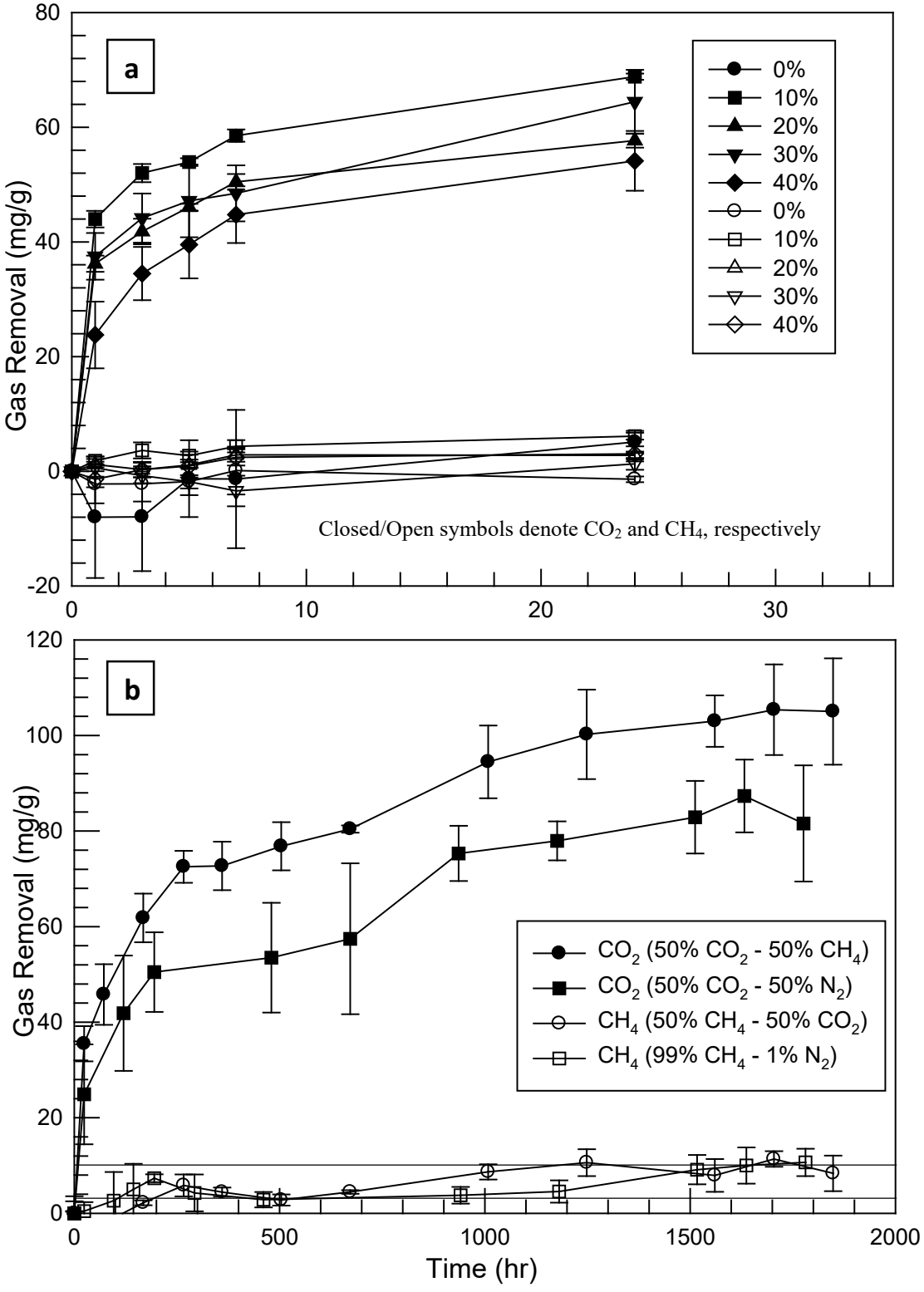
a
Gas Removal (mg/g)
80
60
40
20
0
-20
0
10
20
30
0%
10%
20%
30%
40%
0%
10%
20%
30%
40%
Closed/Open symbols denote CO_2 and CH_4, respectively
b
Gas Removal (mg/g)
120
100
80
60
40
20
0
0
500
1000
1500
2000
Time (hr)
CO_2 (50% CO_2 - 50% CH_4)
CO_2 (50% CO_2 - 50% N_2)
CH_4 (50% CH_4 - 50% CO_2)
CH_4 (99% CH_4 - 1% N_2)

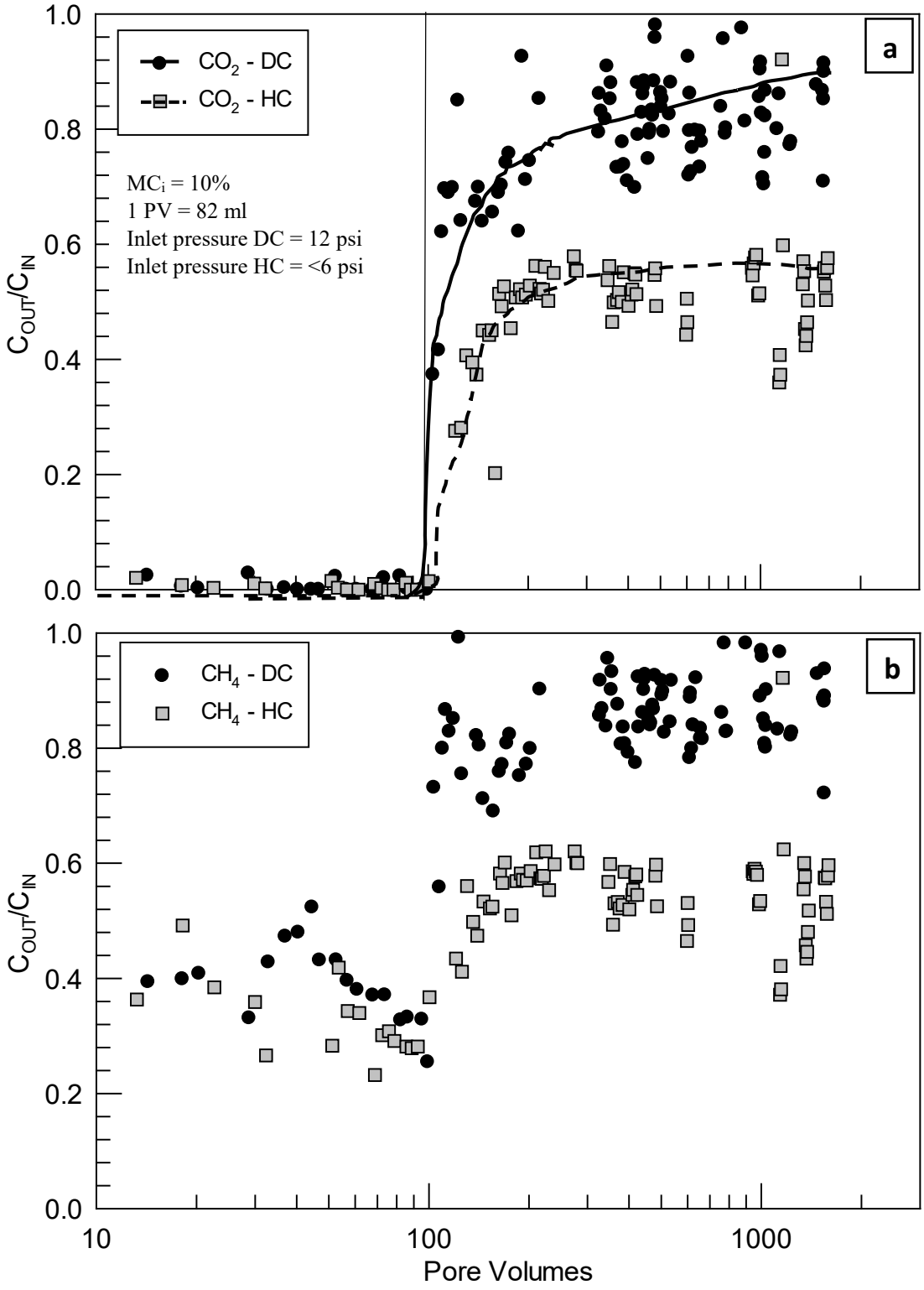
a
CO_2 - DC
CO_2 - HC
MC_i = 10%
1 PV = 82 ml
Inlet pressure DC = 12 psi
Inlet pressure HC = <6 psi
C_{OUT}/C_{IN}
b
CH_4 - DC
CH_4 - HC
C_{OUT}/C_{IN}
Pore Volumes

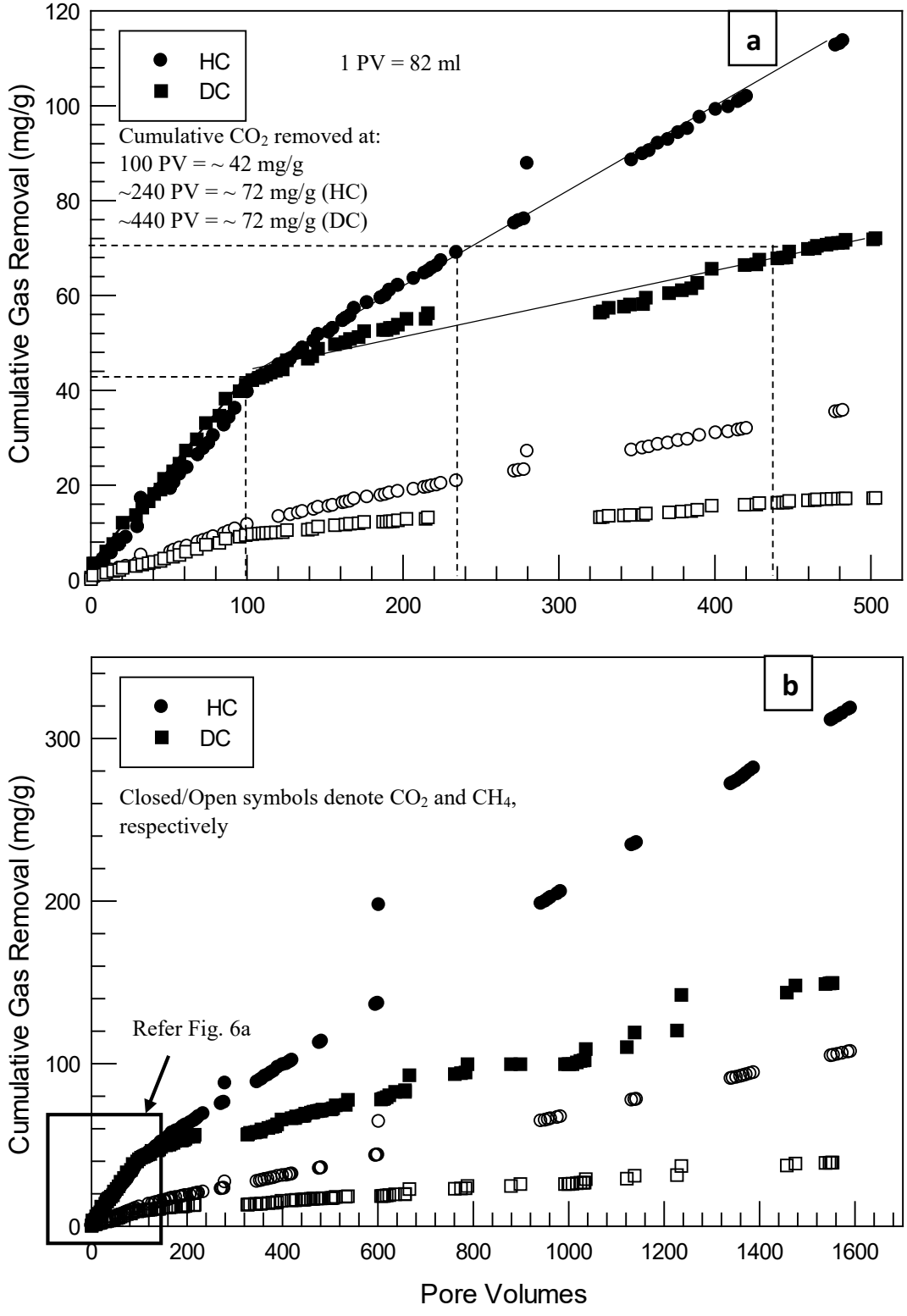
a
HC
DC
1 PV = 82 ml
Cumulative CO_2 removed at:
100 PV = ~ 42 mg/g
~240 PV = ~ 72 mg/g (HC)
~440 PV = ~ 72 mg/g (DC)
Cumulative Gas Removal (mg/g)
b
HC
DC
Closed/Open symbols denote CO_2 and CH_4, respectively
Refer Fig. 6a
Cumulative Gas Removal (mg/g)
Pore Volumes

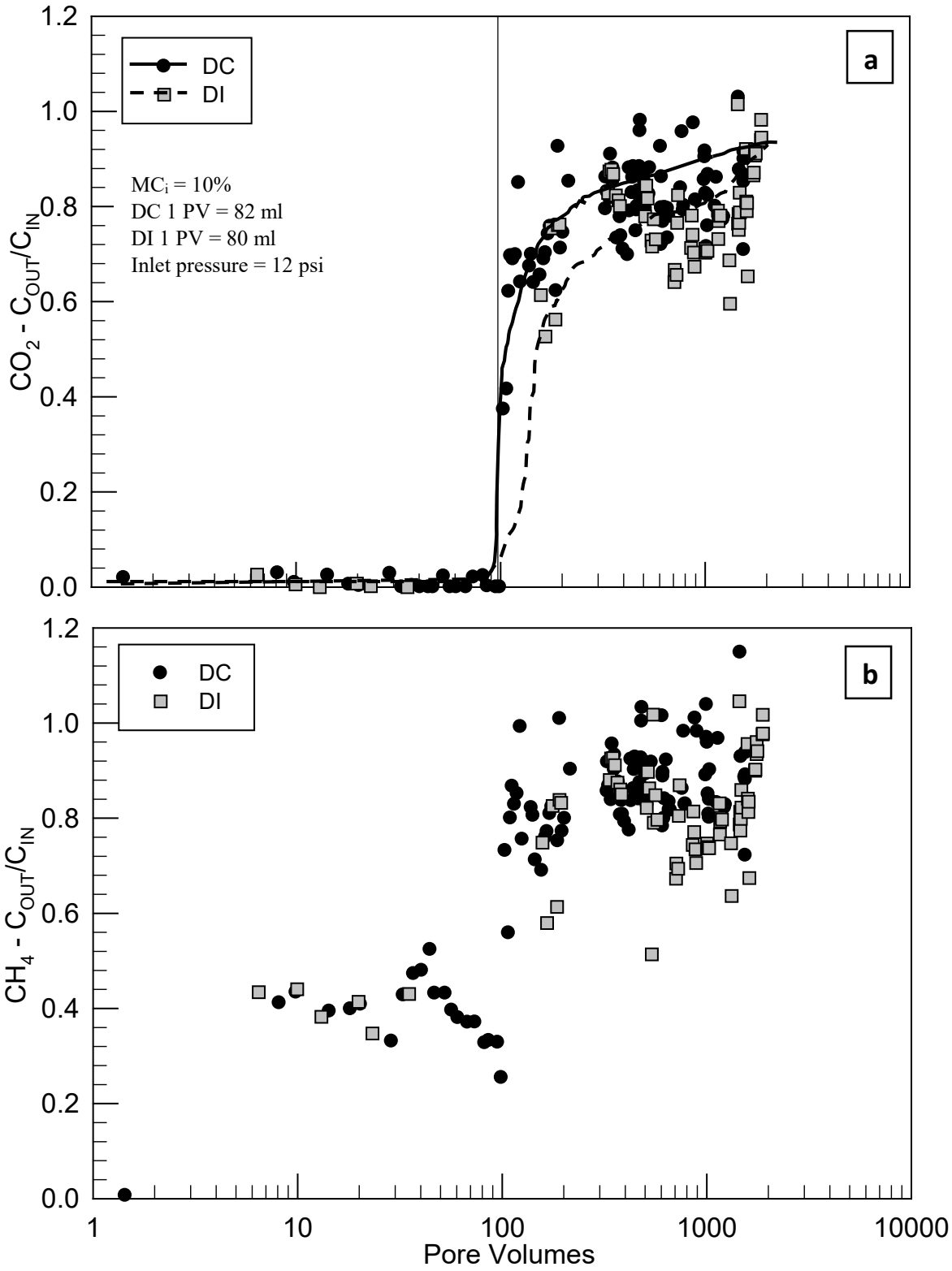
a
DC
DI
MC$_i$ = 10%
DC 1 PV = 82 ml
DI 1 PV = 80 ml
Inlet pressure = 12 psi
CO$_2$ - C$_{OUT}$/C$_{IN}$
b
CH$_4$ - C$_{OUT}$/C$_{IN}$
Pore Volumes
0.0
0.2
0.4
0.6
0.8
1.0
1.2
1
10
100
1000
10000

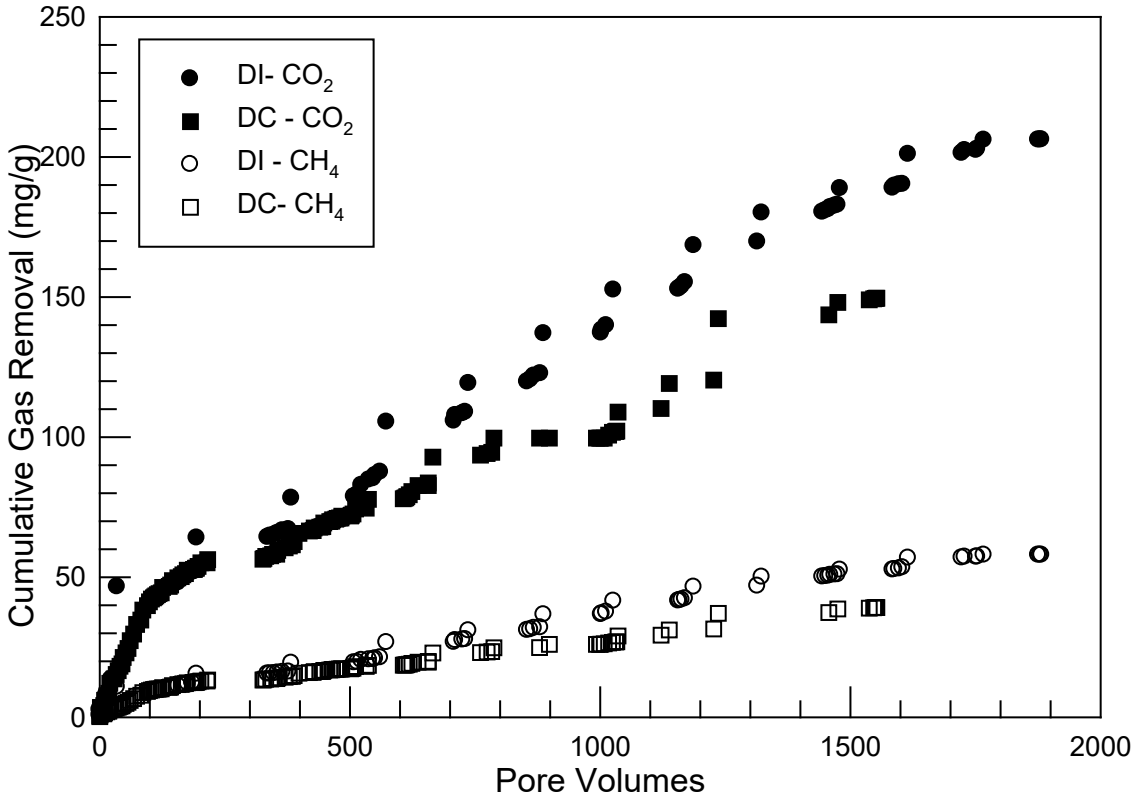
DI- CO_2
DC - CO_2
DI - CH_4
DC- CH_4
Cumulative Gas Removal (mg/g)
Pore Volumes
0
50
100
150
200
250
0
500
1000
1500
2000

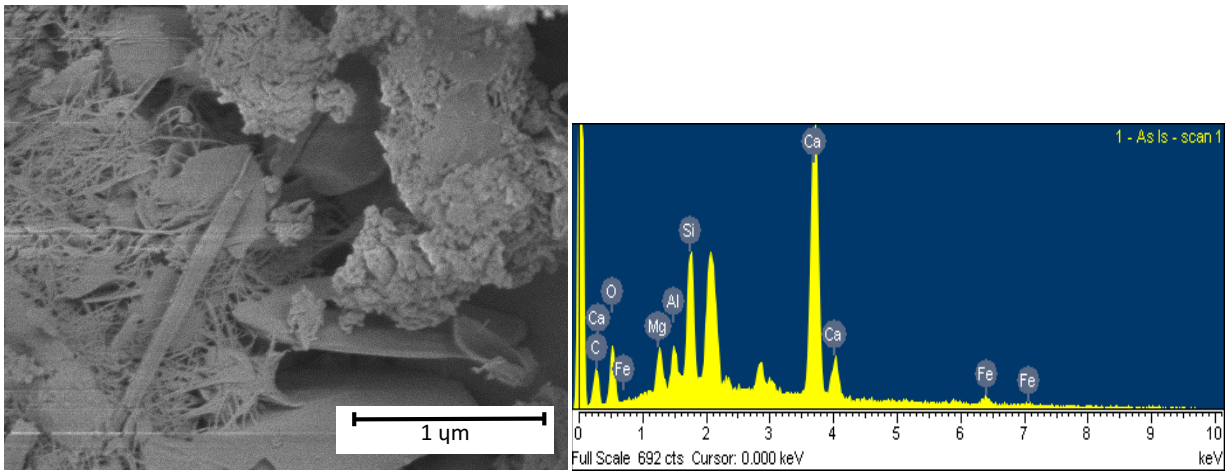

18000x magnification

(a)

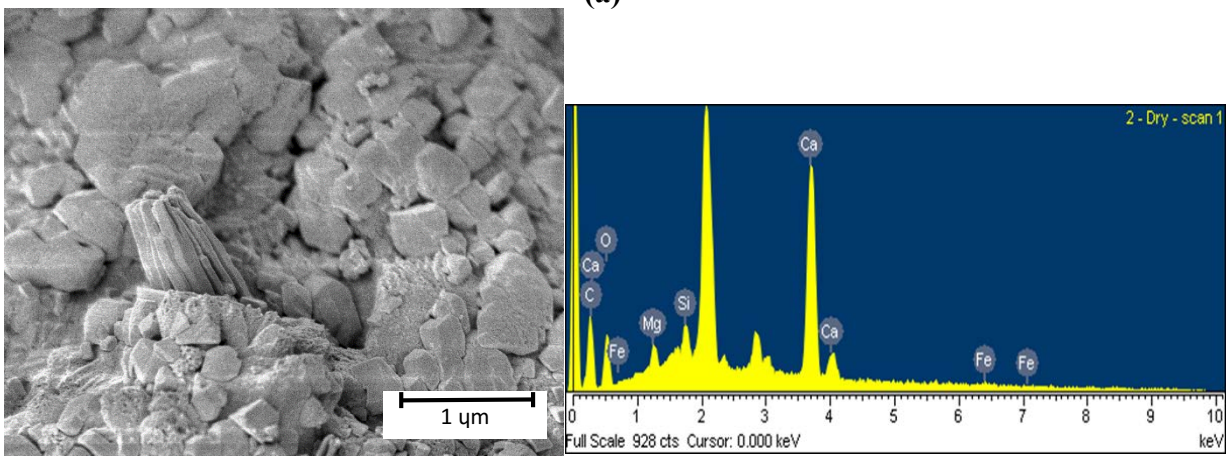

13000x magnification

(b)

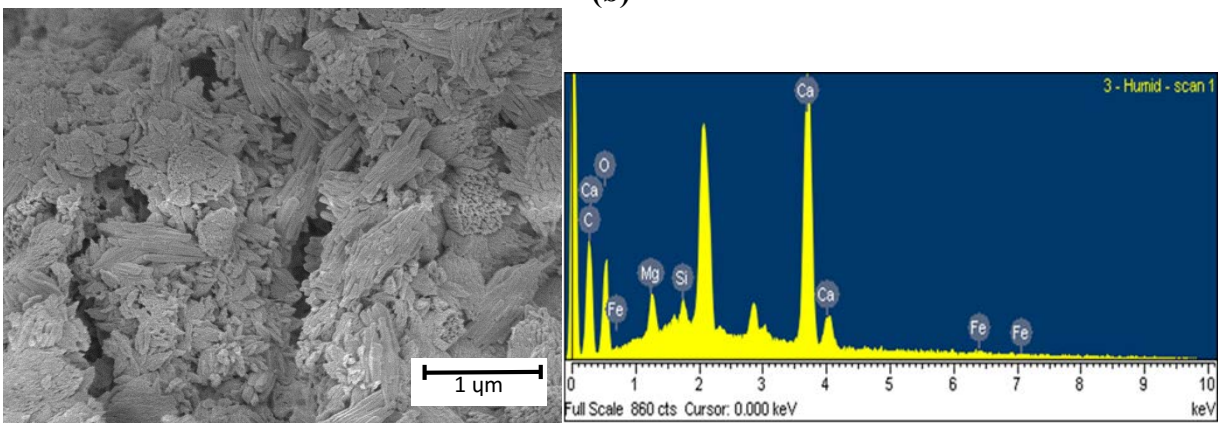

11000x magnification

(c)